nature microbiology

SUPPLEMENTARY INFORMATION

https://doi.org/10.1038/s41564-019-0529-z

In the format provided by the authors and unedited.

A viral kinase counteracts in vivo restriction of murine cytomegalovirus by SAMHD1

Janina Deutschmann[1], Andrea Schneider[2], Iris Gruska[3], Barbara Vetter[3], Dominique Thomas[4], Melissa Kießling[1], Sabine Wittmann[1], Alexandra Herrmann[1], Michael Schindler[5], Jens Milbradt[1], Nerea Ferreirós[4,6], Thomas H. Winkler[2], Lüder Wiebusch[3] and Thomas Gramberg[1]*

[1]Institute of Clinical and Molecular Virology, Friedrich-Alexander University Erlangen-Nürnberg, Erlangen, Germany. [2]Chair of Genetics, Department of Biology, Nikolaus-Fiebiger-Center for Molecular Medicine, Friedrich-Alexander-University Erlangen-Nürnberg, Erlangen, Germany. [3]Laboratory of Molecular Pediatrics, Department of Pediatric Oncology, Hematology and Stem Cell Transplantation, Charité Universitätsmedizin, Berlin, Germany. [4]Pharmazentrum Frankfurt/ZAFES, Institute of Clinical Pharmacology, Goethe University, Frankfurt, Germany. [5]Institute for Medical Virology, University Hospital Tübingen, Tübingen, Germany. [6]Project Group Translational Medicine and Pharmacology TMP, Fraunhofer Institute for Molecular Biology and Applied Ecology IME, Frankfurt, Germany. *e-mail: thomas.gramberg@fau.de

SUPPLEMENTARY INFORMATION

A viral kinase counteracts *in vivo* restriction of murine cytomegalovirus by SAMHD1

Janina Deutschmann[1], Andrea Schneider[2], Iris Gruska[6], Barbara Vetter[6], Dominique Thomas[3], Melissa Kießling[1], Sabine Wittmann[1], Alexandra Herrmann[1], Michael Schindler[4], Jens Milbradt[1], Nerea Ferreirós[3,5], Thomas H. Winkler[2], Lüder Wiebusch[6], Thomas Gramberg[1*]

[1]Institute of Clinical and Molecular Virology, Friedrich-Alexander University Erlangen-Nürnberg, 91054 Erlangen, Germany. [2]Chair of Genetics, Department of Biology, Nikolaus-Fiebiger-Center for Molecular Medicine, Friedrich-Alexander-University Erlangen-Nürnberg, 91054 Erlangen, Germany. [3]pharmazentrum frankfurt/ZAFES, Institute of Clinical Pharmacology, Goethe University, 60590 Frankfurt, Germany. [4]Institute for Medical Virology, University Hospital Tübingen, 72076 Tübingen, Germany. [5]Fraunhofer Institute for Molecular Biology and Applied Ecology IME, Project Group Translational Medicine and Pharmacology TMP, 60590 Frankfurt, Germany. [6]Laboratory of Molecular Pediatrics, Department of Pediatric Oncology, Hematology and Stem Cell Transplantation, Charité Universitätsmedizin, 10117 Berlin, Germany. *email: thomas.gramberg@fau.de

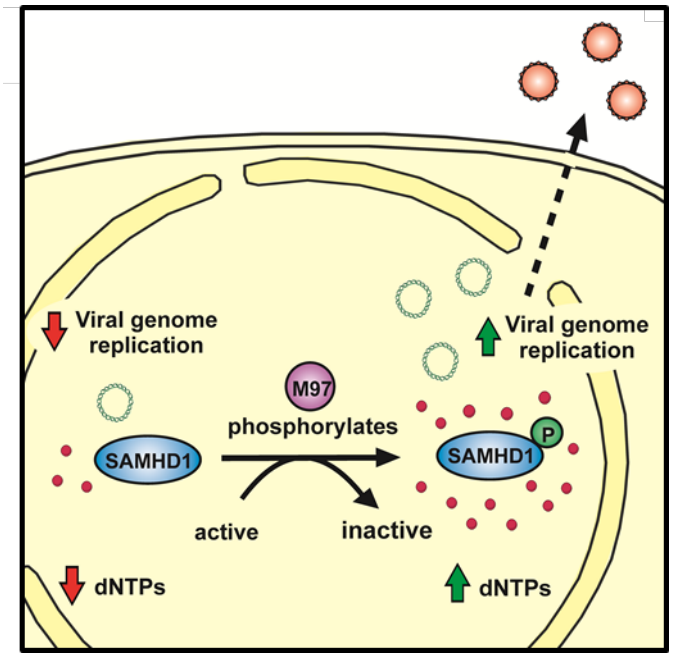

Supplementary Figure S1. Model of the interaction between host factor SAMHD1 and the viral kinase M97. As important component of dNTP metabolism, active SAMHD1 is responsible for low intracellular dNTP concentration. Our data indicate that upon MCMV infection, SAMHD1 is inactivated through phosphorylation by the viral kinase M97, leading to increased dNTP levels and consequently to elevated viral genome replication and production of infectious virus.

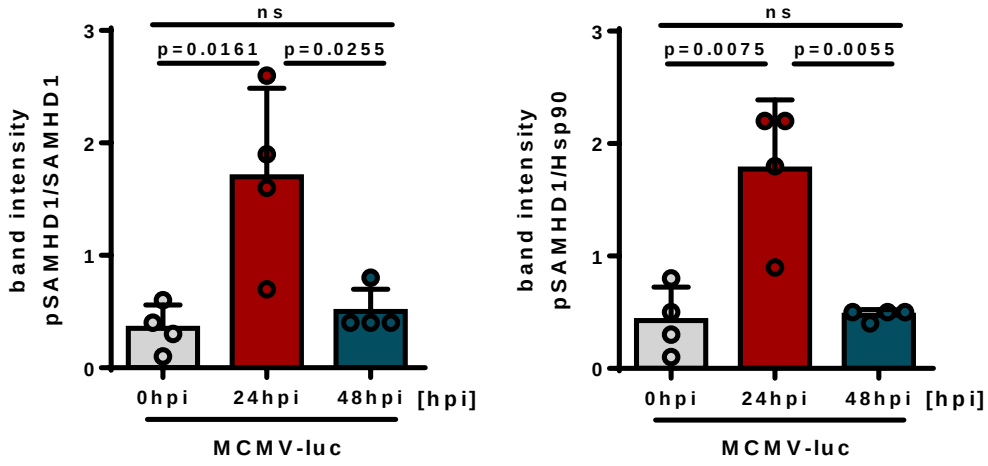

Supplementary Figure S2. Quantification of SAMHD1 phosphorylation upon MCMV-luc infection in BMDMs (Fig. 2c). Immunoblot signals were quantified using AIDA software. Band intensity of phospho-SAMHD1 was normalized either to SAMHD1 or the housekeeping gene Hsp90. Columns depict the average of four signals ± SD. Statistical analysis was performed using an unpaired, two-tailed t-test. hpi: hours postinfection. ns: not significant.

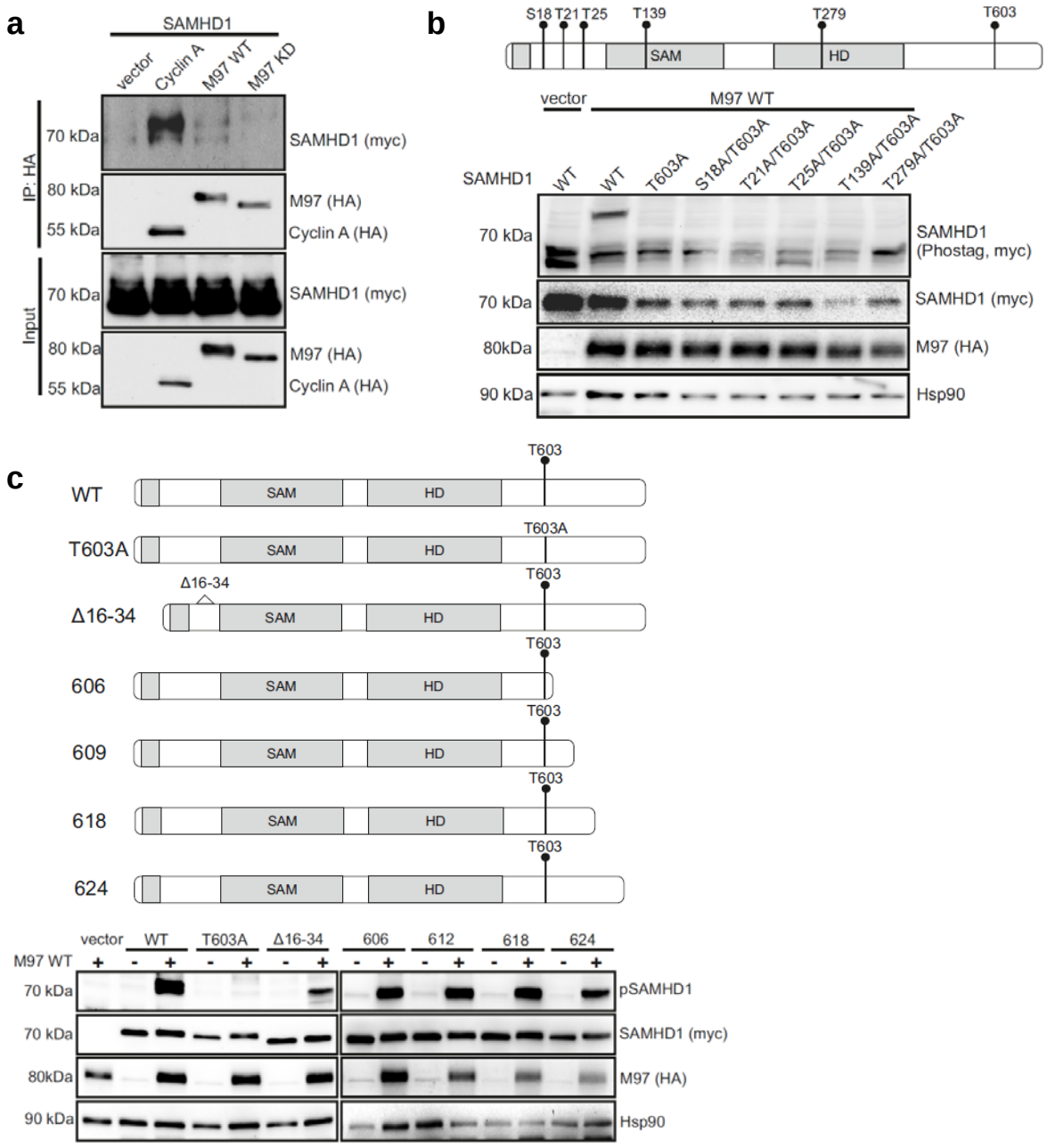

Supplementary Figure S3. Interaction between SAMHD1 and viral kinase M97. (a) Coexpression and immunoprecipitation of empty vector, HA-cyclin A, HA-M97 WT, and HA-M97 KD and SAMHD1-myc in HEK 293T cells. Proteins were precipitated with anti-HA antibodies (HA), bound SAMHD1-myc was detected by anti-myc (myc) antibodies. One of two independent assays is shown. (b) Overview and Phos-tag blot of serine/threonine mutants of SAMHD1-myc co-expressed with HA-M97 in 3T3 cells. Membranes were probed with antibodies against phospho-T603 SAMHD1 (pSAMHD1), SAMHD1 (myc), M97 (HA), and Hsp90. One of two independent western blots is shown. (c) Overview of M97-interacting mutants of SAMHD1 and immunoblot analysis of coexpression with M97 in 3T3 cells. Phosphorylation of SAMHD1 mutants was analyzed as surrogate for interaction with M97.

Membranes were probed with antibodies against phospho-SAMHD1 (pSAMHD1), SAMHD1 variants (myc), M97 (HA), and Hsp90. One of two independent blots is shown.

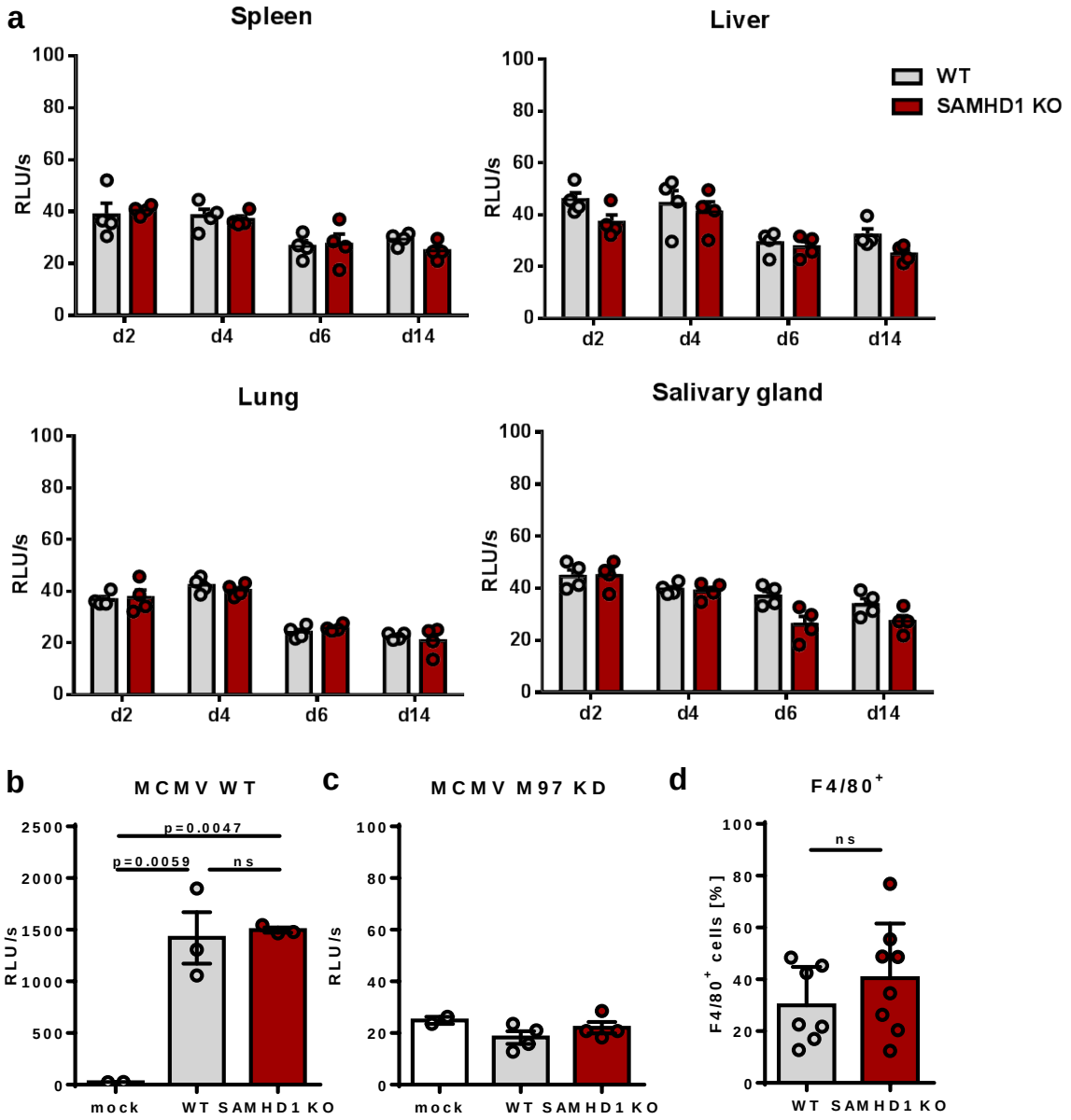

Supplementary Figure S4. MCMV M97 KD *in vivo* infections and analysis of peritoneal macrophages. (a) Analysis of MCMV M97 KD-luc infected organs of C57BL/6 (WT) and SAMHD1 KO mice. For each time point, four WT and SAMHD1 KO mice (n=4) were infected intravenously with MCMV M97 KD-luc (1 x 10^6 PFU/ mouse). On day 2, 4, 6, and 14 postinfection, spleen, lung, liver, and salivary glands were isolated and homogenized. Lysates were normalized using BCA assays, luciferase activity was determined in duplicates as surrogate for viral infection. One of two independent experiments is shown, columns represent mean relative light units (RLU)/s ± SEM. C57BL/6 and SAMHD1 KO mice were infected intraperitoneal with (b) MCMV-luc (1 x 10^5 PFU/ mouse; n=3) or (c) MCMV M97 KD-luc (1 x 10^5 PFU/ mouse; n=4). Cells were isolated 6 dpi, lysed, and analyzed by luciferase assay in quadruplicates. Columns represent mean relative light units (RLU)/s ± SEM. Statistical analysis was performed by one-way ANOVA followed by Tukey's multiple

comparisons test. (d) Isolated peritoneal cells were probed with F4/80-APC antibody and quantified by flow cytometry. Columns (n=8) represent the mean percentage of viable F4/80-positive cells. Statistics were analyzed using an unpaired, two-tailed t-test. ns: not significant.

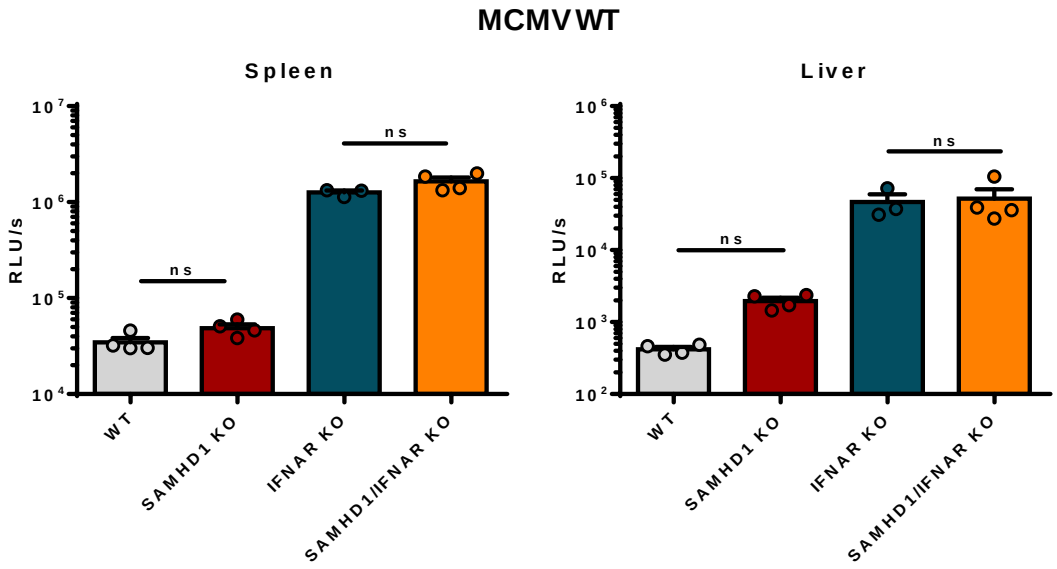

Supplementary Figure S5. MCMV WT *in vivo* infections. Analysis of MCMV-luc WT infected organs of C57BL/6 (WT), SAMHD1 KO, IFNAR KO and SAMHD1/IFNAR KO mice (n=4, IFNAR KO n=3). Mice were infected intravenously with MCMV-luc WT (1 x 10^5 PFU/ mouse). On day 4 postinfection, spleen and liver were isolated and homogenized. Lysates were normalized using BCA assays, luciferase activity was determined in duplicates as surrogate for viral infection. Columns show the average relative light units (RLU)/s ± SEM. One of two independent assays is shown. Statistical analysis was performed using one-way ANOVA followed by Tukey's multiple comparisons test. ns: not significant.

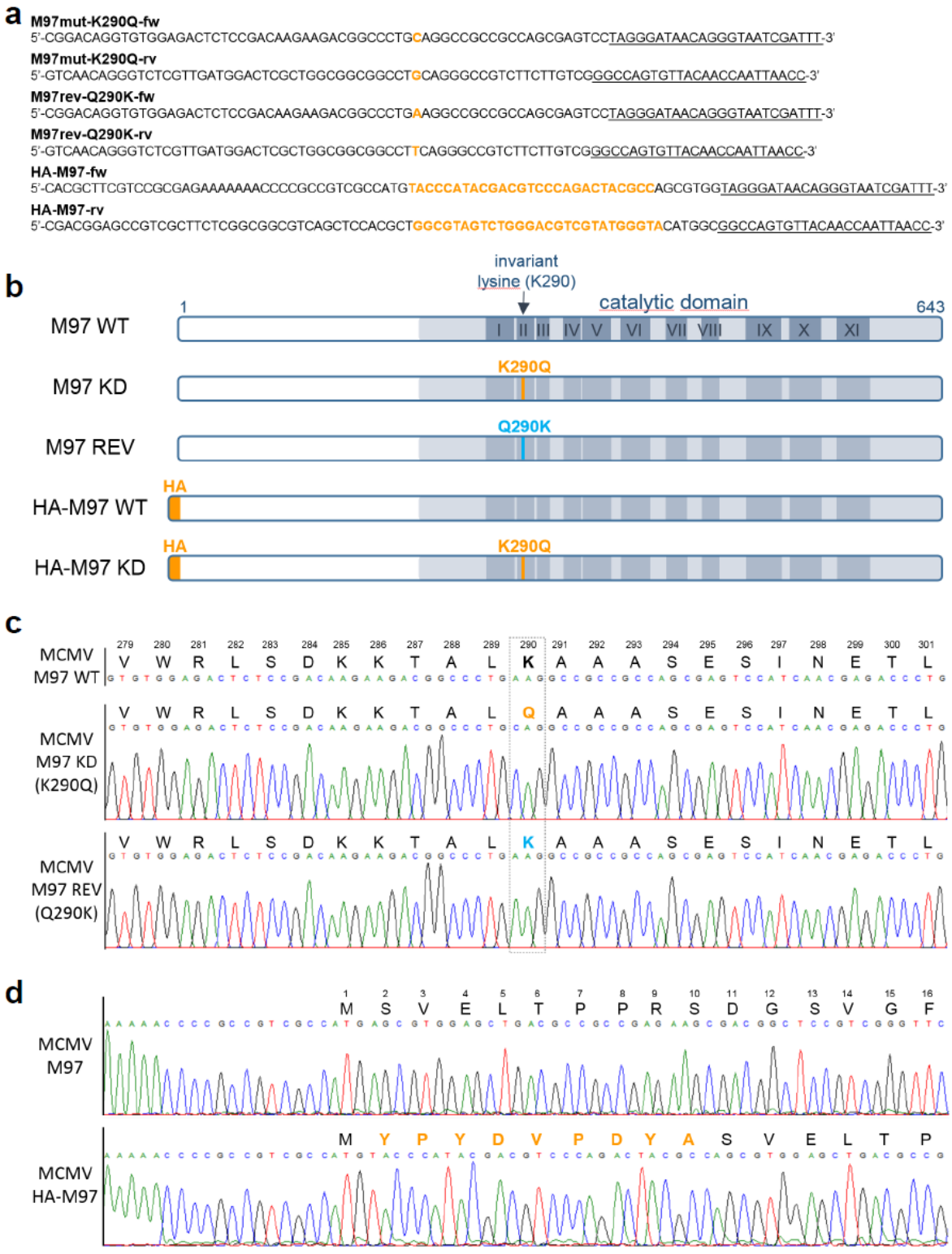

Supplementary Figure S6. Construction of recombinant viruses. (a) Sequences of DNA oligonucleotide primers used for seamless BAC mutagenesis of MCMV-ΔM157-luc repaired-MCK2fl (MCMV WT). Nucleotides changing the parental viral sequence are highlighted in orange letters. Sequences annealing to pEPkanS2 are underlined. (b) Schematic overview of alterations introduced into M97 kinase. Conserved sequence stretches present in the

catalytic domains of all kinases are marked with roman numerals according to Hanks *et al*.[36]. The invariant lysine in subdomain II is essential for catalytic activity and was mutated as indicated [37]. (c) DNA sequence chromatograms resulting from Sanger sequencing of the M97 gene region from the indicated recombinant viruses. (d) DNA sequence chromatograms resulting from Sanger sequencing of the HA-tag from the indicated recombinant viruses.

SI Reference list

36 Hanks, S. K., Quinn, A. M. & Hunter, T. The protein kinase family: conserved features and deduced phylogeny of the catalytic domains. Science 241, 42-52 (1988).

37 Carrera, A. C., Alexandrov, K. & Roberts, T. M. The conserved lysine of the catalytic domain of protein kinases is actively involved in the phosphotransfer reaction and not required for anchoring ATP. Proc Natl Acad Sci U S A 90, 442-446, doi:10.1073/pnas.90.2.442 (1993).

Raw immunoblot data

Fig. 2c

Left Blot

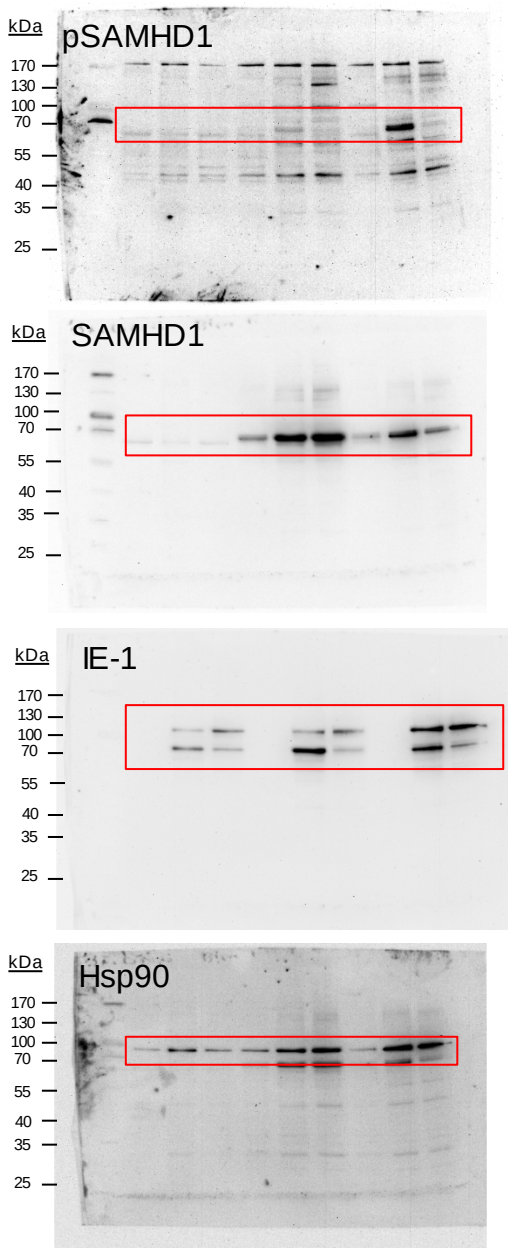

Right Blot

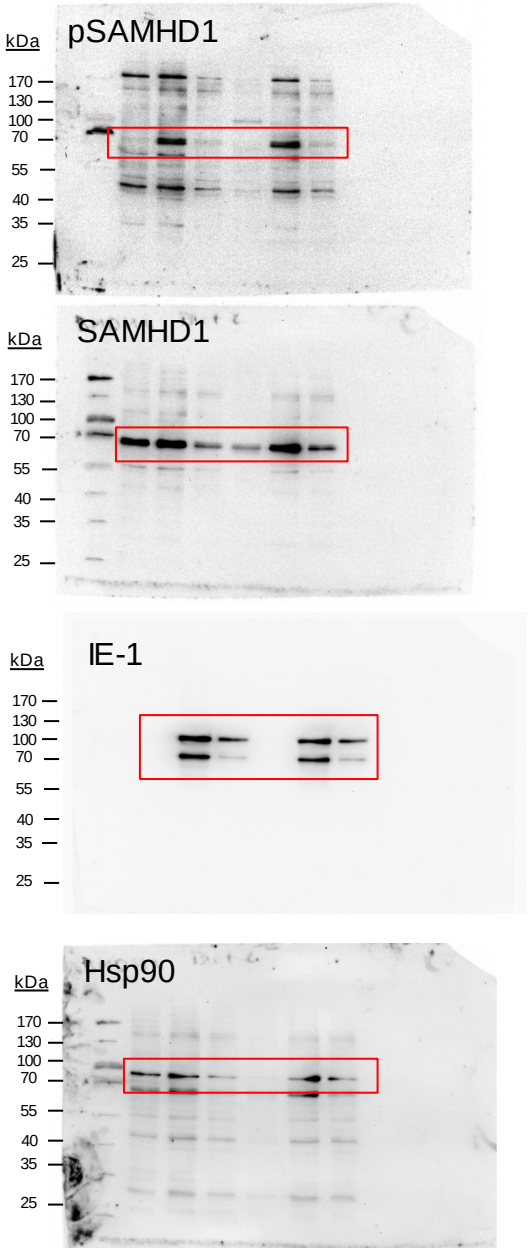

Fig. 3a

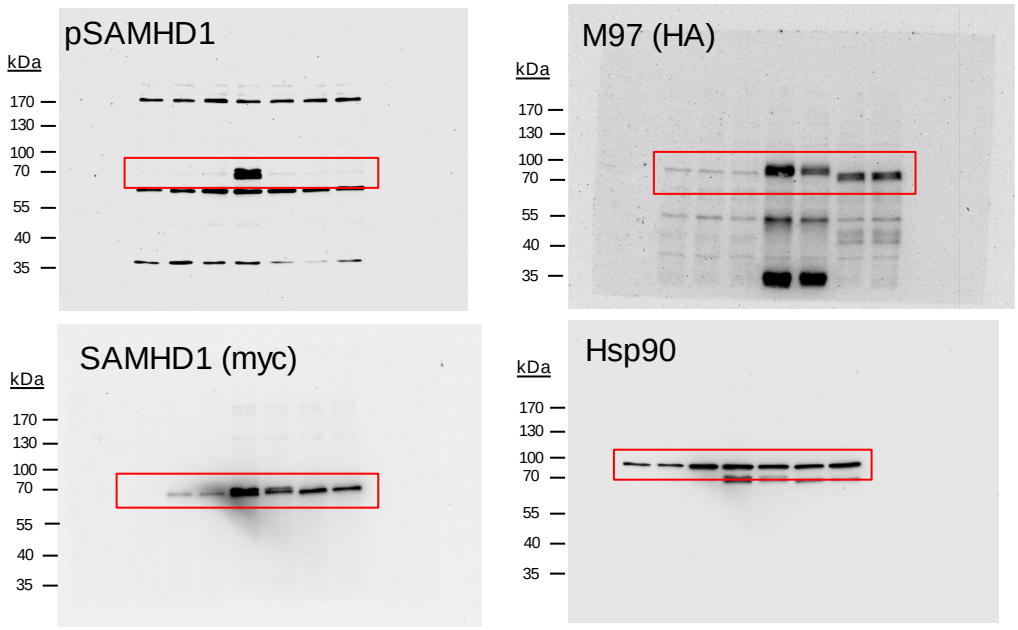
pSAMHD1
M97 (HA)
SAMHD1 (myc)
Hsp90
kDa
170
130
100
70
55
40
35

Fig. 3b

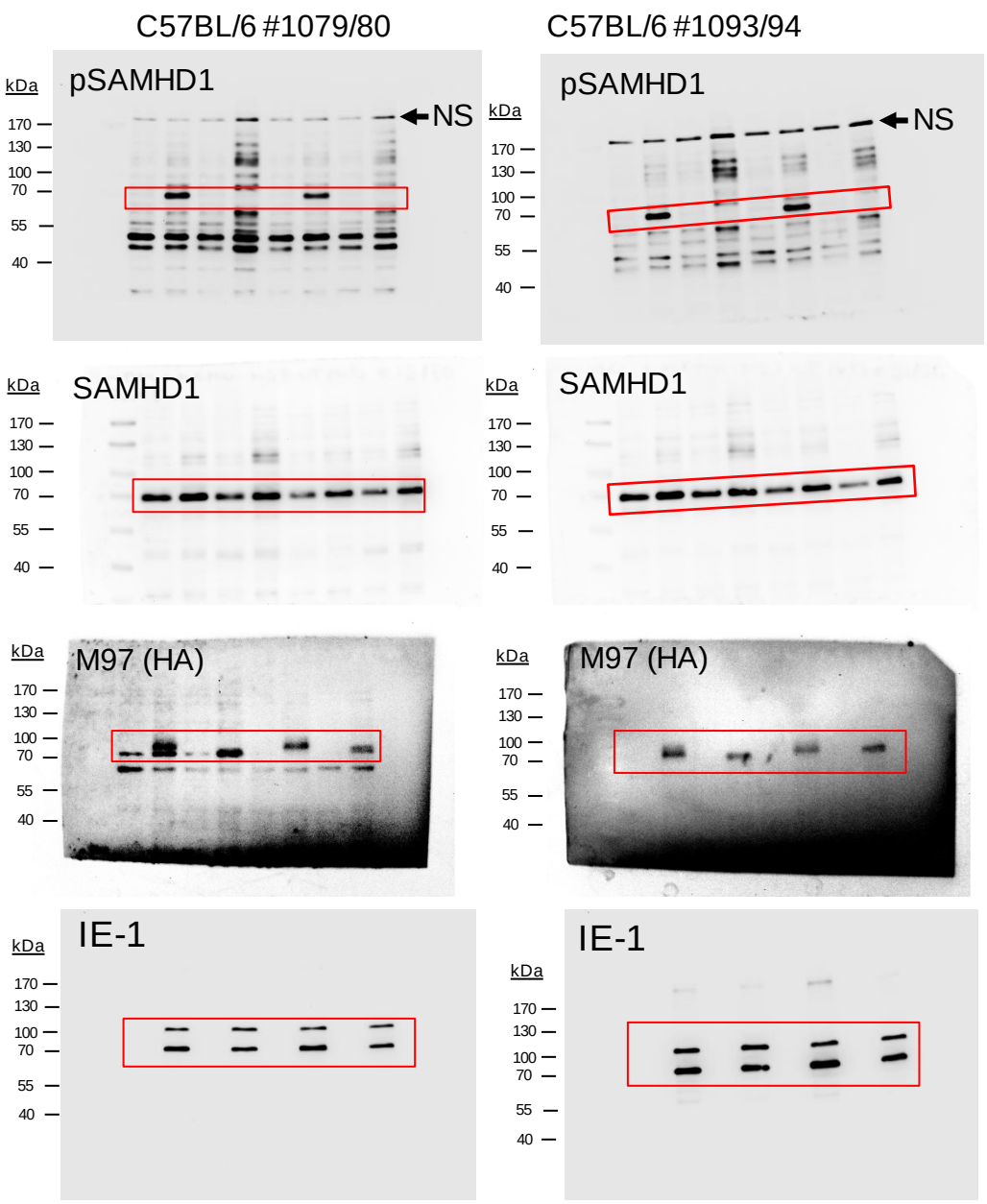
C57BL/6 #1079/80
C57BL/6 #1093/94
pSAMHD1
NS
SAMHD1
M97 (HA)
IE-1
kDa
170
130
100
70
55
40

Fig. 3c MCMV WT

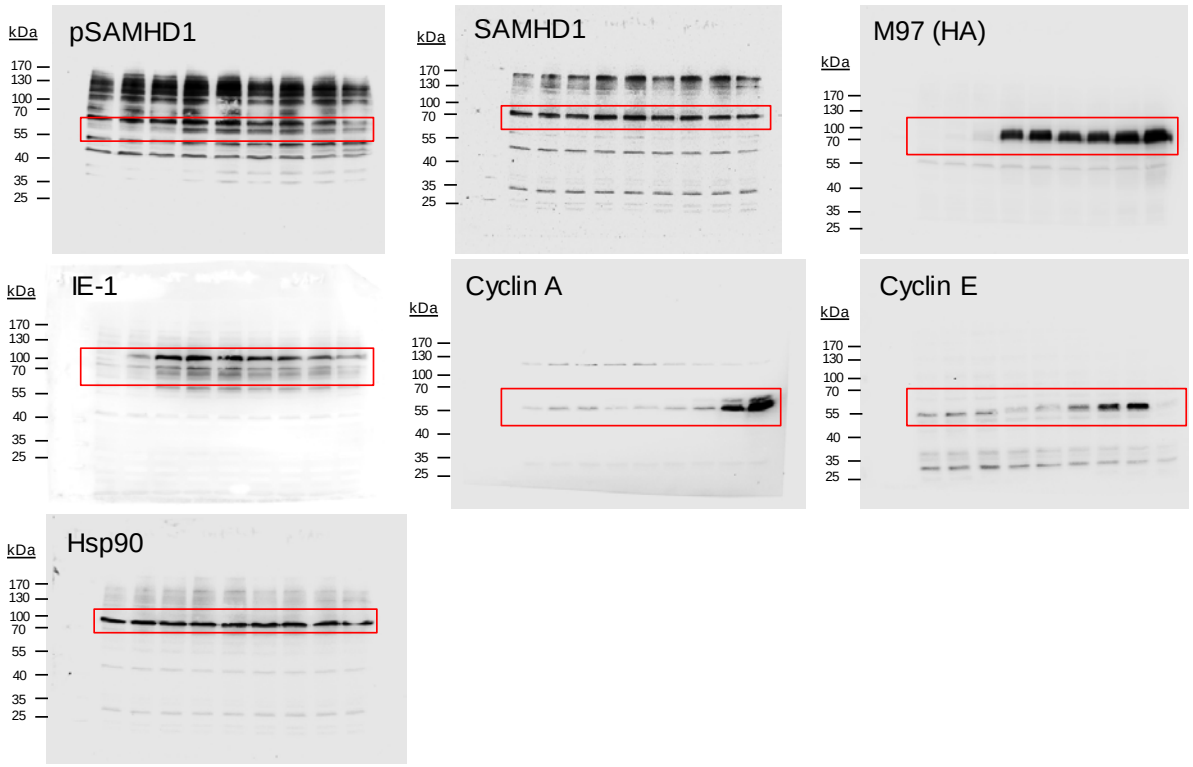

MCMV M97 KD

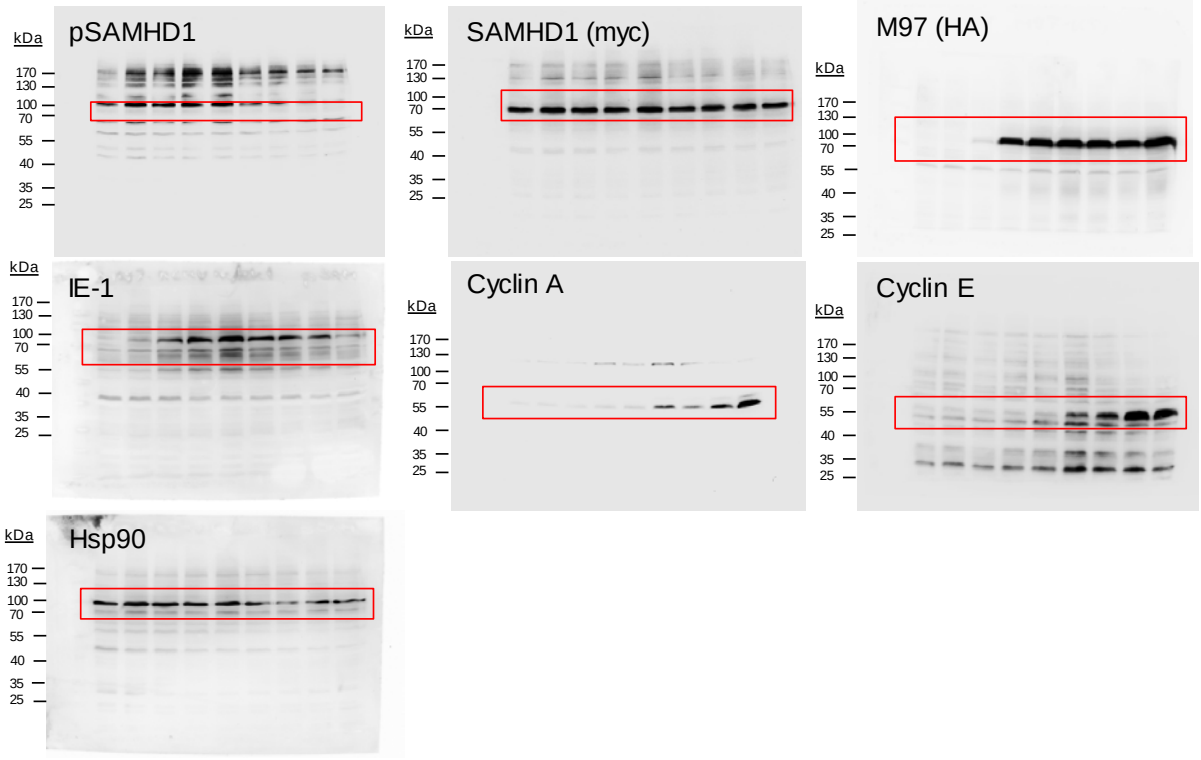

Fig. 3d

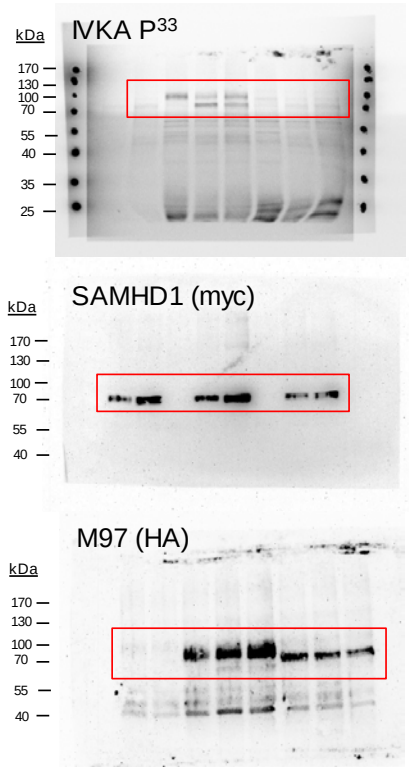

Fig. 3e

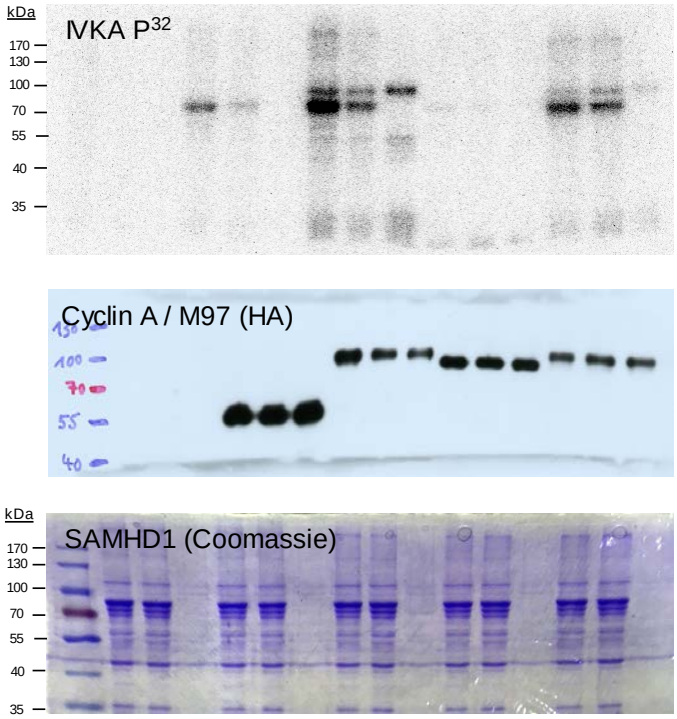

Fig. 4b

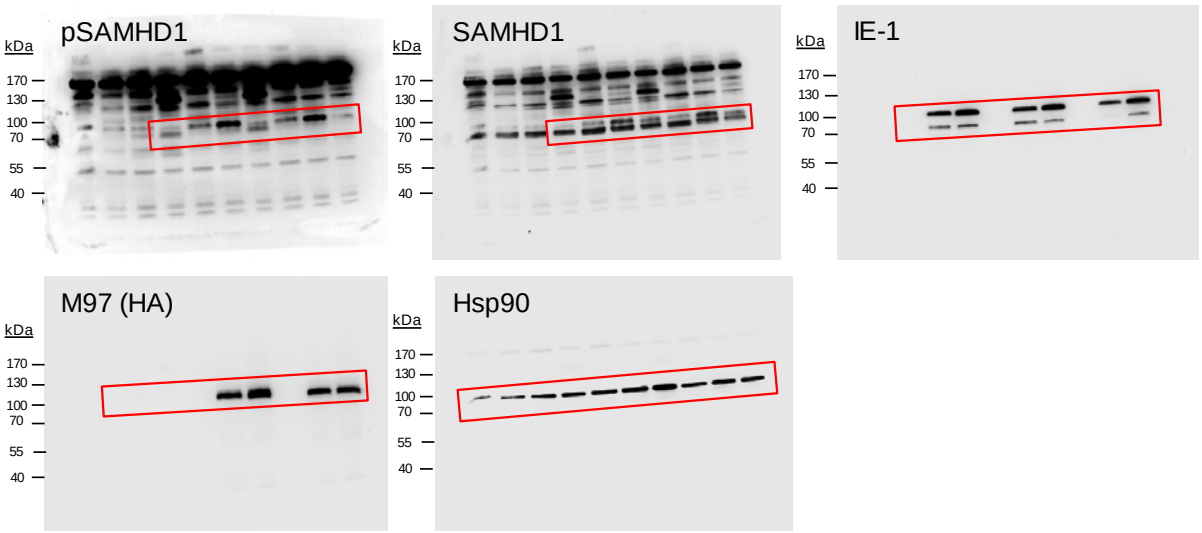

Fig. 6a

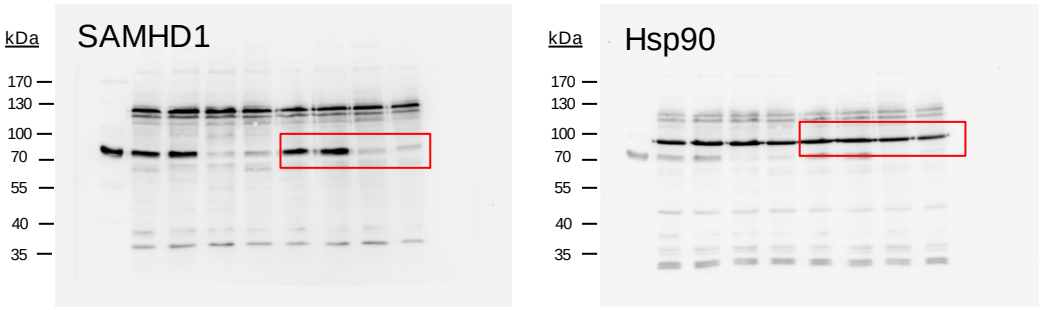

Fig. 6f

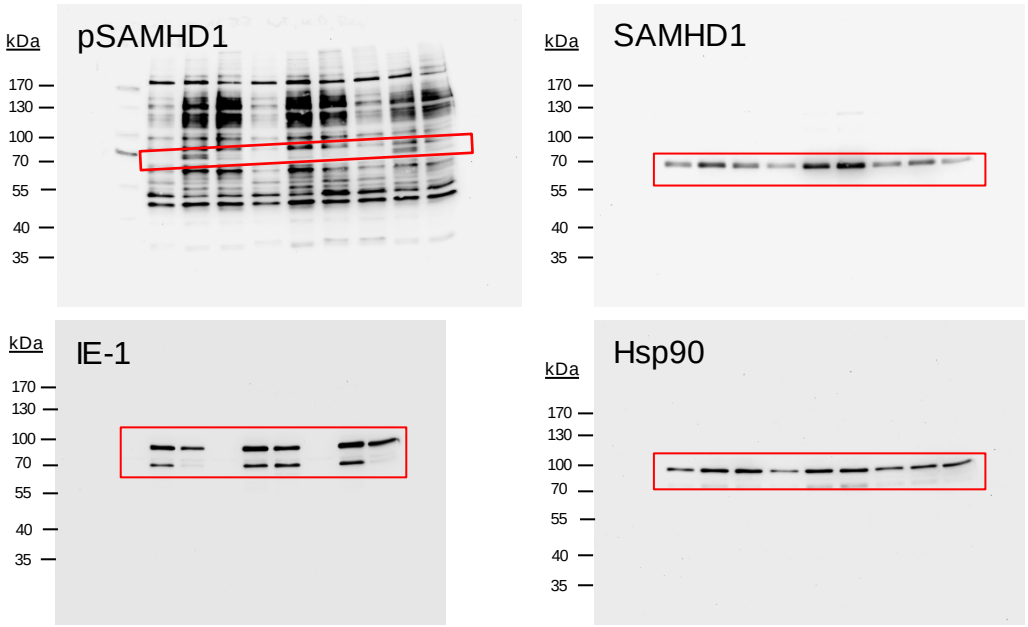

Fig. 6g

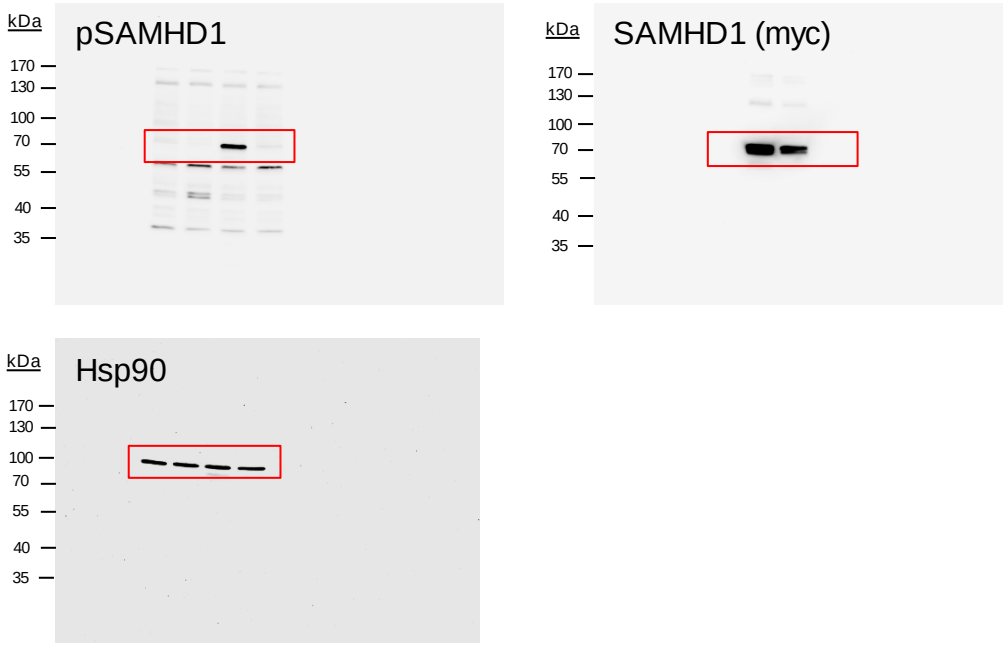

S2b

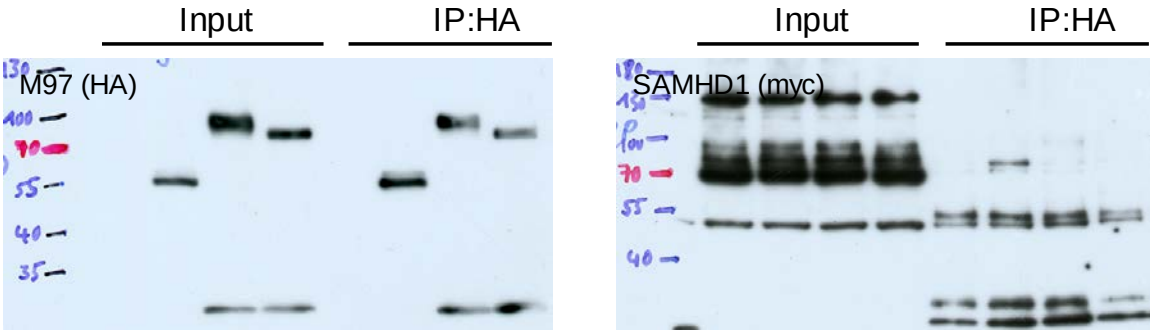
Input
IP:HA
M97 (HA)
Input
IP:HA
SAMHD1 (myc)

S2c

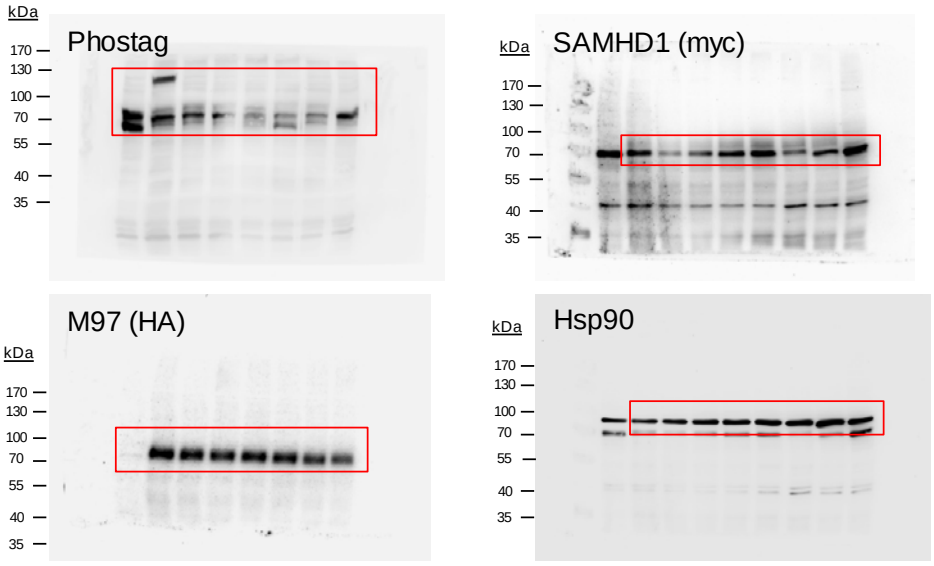
kDa
170
130
100
70
55
40
35
Phostag
kDa
SAMHD1 (myc)
M97 (HA)
kDa
Hsp90

S2d

Left Blot

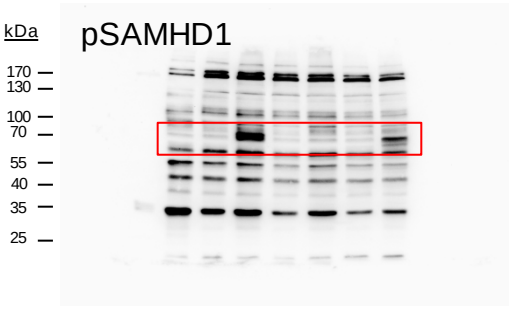

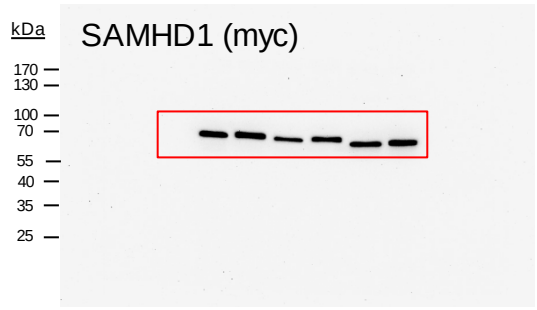

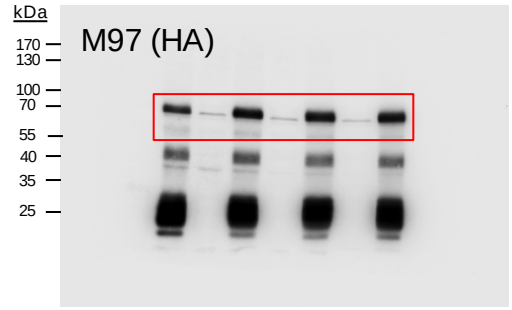

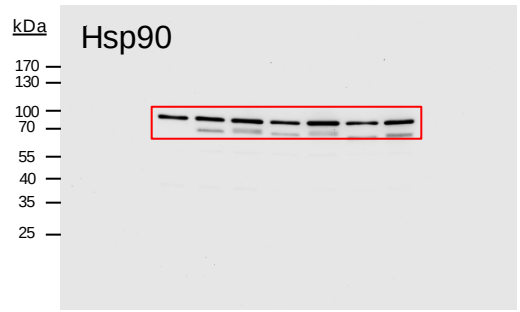

Right Blot